Journal of Ovonic Research Vol. 6, No. 1, January 2010, p. 1 - 11

OPTICAL AND ELECTRICAL INVESTIGATIONS ON γ-MnS THIN FILMS

M. DHANAM*, B.KAVITHA, M. SHANMUGA PRIYA
PG & Research Department of Physics, Kongunadu Arts and Science College, Coimbatore, Tamilnadu, India-641029.

γ-MnS thin films have been prepared from three chemical baths by optimizing various preparatory conditions. Transmittance spectra analysis helped to establish the type of transition as direct allowed and the optical parameters are evaluated and reported. The room-temperature as well as high temperature conduction mechanisms were identified and the parameters are reported and discussed in this paper.

(Received January 20, 2010; February 17, 2010)

Keywords: CBD, Absorbance, Transmittance, PL Spectra

1. Introduction

Materials containing manganese are interesting because of their applications in many areas of modern technology. MnS is a wide gap [band gap energy, Eg ~ 3.1eV] VIIB – VIA magnetic semiconductor. MnS is a DMS (Dilute Magnetic Semiconductors) material having potential use in short wavelength optoelectronics devices. MnS occurs in three forms: the stable green α-MnS with rock salt type structure, pink metastable tetrahedral structures (β-MnS-sphalarite type) and pink (γ-MnS-Wurtzite type). Both tetrahedrally coordinated β and γ forms can only exist in a low temperature range and will transform irreversibly to the octahedrally coordinated stable α form at 100-400˚C. Both metastable states are orange/pink coloured. The melting point and density of MnS are 1610°C and 4000 Kg/m^3 respectively.

MnS is used in solar cell applications as a window/buffer material [1]. MnS is especially used in mixing with Zn and Cd to form (Zn, Mn) S and (Cd, Mn) S. MnS has been extensively studied because of their outstanding magneto-optical properties [2]. MnS thin films have an interesting combination of magnetism and semiconductivity. In DMS, the band electrons and holes strongly interact with the localized magnetic moments and cause a variety of interesting phenomena [2-3]. These DMS materials have gained much interest because of their application as blue green light emitters [4,5]. These materials could provide a new type of control of conduction and spin which is an important property of spintronics applications. The metastable form can be easily prepared from an aqueous solution [6].

2. Experimental details

The deposition of MnS thin films is based on the reaction of Mn^{2+} and S^{2-} ions in deionized water solution. Chemicals used for the deposition of MnS thin films are manganese acetate, triethylamine, ammonium chloride, hydrazine hydrate and thioacetamide. For the preparation of MnS thin films, 10 ml (1mol l^{-1}) manganese acetate solution was taken in a 100ml beaker to which 1ml triethylamine (98%) and 10 ml (1 M) NH_4Cl (1 mol l^{-1}) were added successively. After stirring for several minutes the solution becomes clear and homogenous. Then under continuous

*Corresponding author-mail: monikagokul@yahoo.com

stirring, 0.2ml of hydrazine hydrate (80%) was mixed and followed by 10 ml of thioacetamide solution (1 mol l^{-1}). Deionized water was added to make the volume to 80ml.

PH of the reaction mixture was varied from 2 to 7 and it was optimizes as 5. The depositions were carried out in water bath at different temperatures and uniform films were obtained for the deposition temperature of 60º C and 70º C. The deposition time was varied from 3 hours to 7 hours to obtain MnS films and the time has been optimized as 5 and 6 hours to get films of different thicknesses. Thus the preparative parameters were optimized to obtain good quality MnS thin films. The bath temperature was fixed at an appropriate optimized temperature, pre-treated substrates was vertically inserted into the beaker. After deposition for an optimized deposition time, the substrates were taken out washed with deionized water and dried in air.

Table 1 preparatory condition of γ- MnS thin films of three different chemical baths

Chemical baths	Film Thickness (Å)	Deposition Temperature (˚C)	Deposition Time (Hrs)	pH
Bath 1	4170	70	5	5
Bath 2	5270	70	6	5
Bath 3	5850	60	6	5

3. Result and discussion

a. Optical studies

Fig 1 and Fig 2 show UV-VIS transmittance and absorbance spectra of MnS thin films from three different chemical baths (preparatory conditions of chemical bath are presented in Table1). The transmittance/absorbance spectra of MnS thin films decreases/increases with film thickness irrespective of the chemical bath (Fig 1.a and Fig 2.a). The transmission [1, 4, 6 & 7] and absorption [8-9] spectra of MnS thin films have been analysed by earlier workers. Figures 1.b and 2.b prove that the transmittance and absorbance decreases/increases with deposition temperatures. Comparing the transmission and absorption curves of MnS thin films of 4170Å (deposition temperature-70ºC and deposition time-5 hrs) and 5850 Å (deposition temperature-60ºC and deposition time-6 hrs) it can be concluded that the very similar nature of the two curves may be due to the higher rate of deposition in high temperature. That is the reason for the lesser deposition time (5 hrs) to get uniform and adherent films at 70ºC instead of having deposition time of 6 hrs at 60ºC. Analyzing the transmission and absorbance curves of 5270 Å (deposition temperature-70ºC and deposition time-6 hrs) and 4170Å (deposition temperature-70ºC and deposition time-5 hrs) it can also be concluded that the optimum deposition time is 5 hrs at 70ºC to get smooth film whereas if the deposition time has been increased from 5 hrs to 6 hrs, the thickness increases along with the roughness and that may be the reason for the slight variation of transmission and absorption curves of MnS thin films of thickness 5270 Å.

Plot of $(\alpha h\upsilon)^2$ versus $(h\upsilon)$ for MnS thin films from three chemical baths are shown in Fig. 3. Direct allowed band gap of 3.83 eV to 4.03 eV has been obtained which reveal the presence of direct allowed transitions in the prepared thin films. The bandgap energy is predicted as 3.5eV for pure binary γ-MnS [10]. The estimated bandgap values are much wider that the reported values which proves the absence of impurity electronic levels in the forbidden gap. The observed band gap values are in agreement with early reported values [1,6, 9-11]. The estimated values of the absorption coefficient, extinction coefficient and bandgap energies are presented in Table 2. The decrease in optical parameters with increase in film thickness might be due to the improvement in crystallinity and decreased strain in higher thickness films irrespective of chemical baths [12].

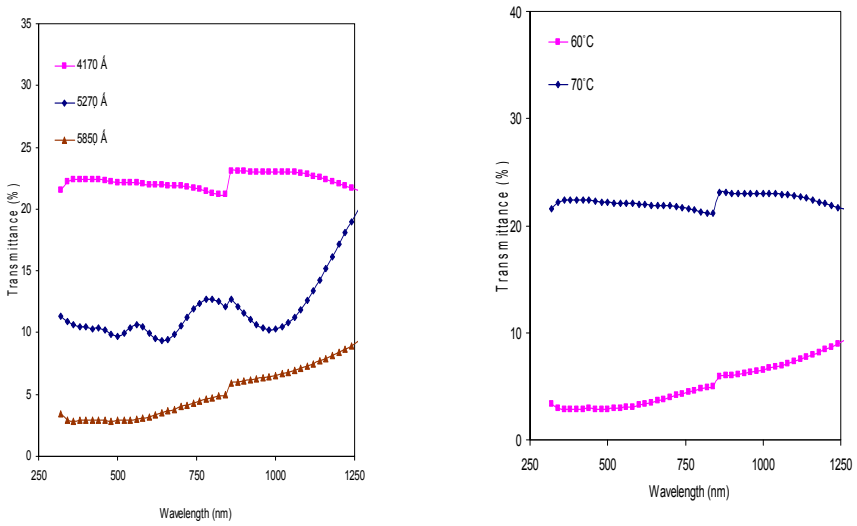

a b

Fig 1.a Transmittance Spectra of γ MnS thin films prepared from three different chemical baths, b. Transmittance Spectra of γ MnS thin films prepared at different deposition temperatures.

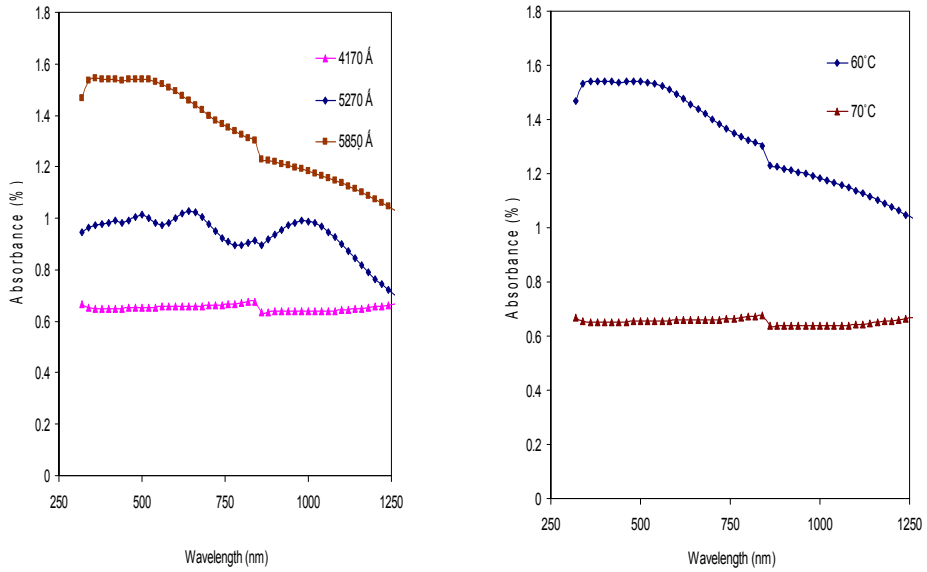

Fig 2.a Absorbance Spectra of γ MnS thin films prepared from three chemical baths. b.Absorbance spectra of γ MnS thin films prepared at different deposition temperature.

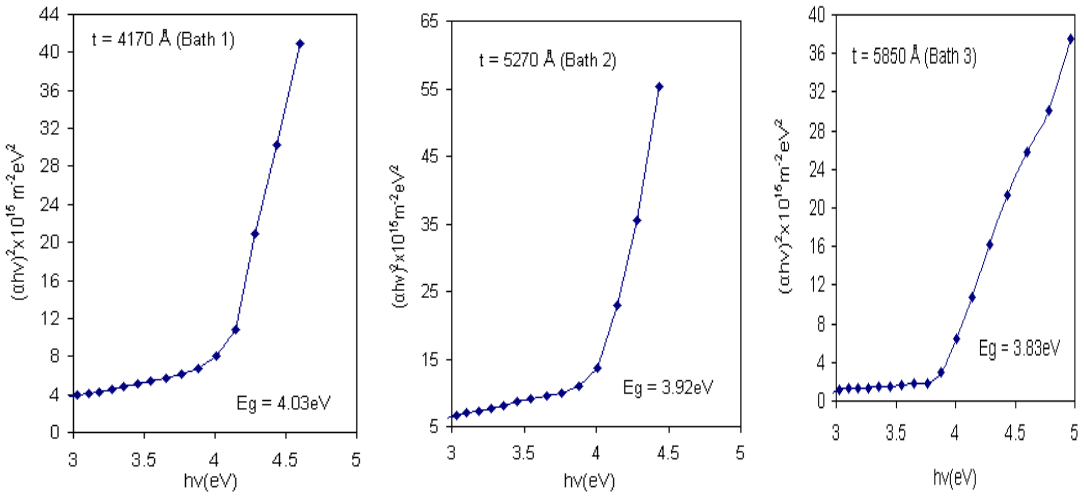

Fig.3. Plot of $(\alpha hv)^2$ vs. hv of γ- MnS thin films.

Table 2 Optical Parameters of γ MnS thin films.

Film Thickness (Å)	Absorbtion Coefficient(α) m^{-1}	Extinction Coefficient(K_f)	Band Gap energy E_g (eV)
	(λ = 5000 Å)		
4170 5270 5850	20.71 8.49 3.61	0.824 0.338 0.144	4.03 3.92 3.83

b. Photoluminescence studies

Fig 4 .a and b show the excitation spectra of MnS thin films with emission intensities of 698 and 700 nm respectively whereas Fig 5.a and b show the room temperature photoluminescence (PL) spectra for the excitation energies 3.5eV and 3.9eV respectively.

It has been found that the absorption peaks occur in the wavelength range of 320–350nm and emission peak occurs at a higher wavelength (approximately at 700nm) than that of the absorption spectrum. This phenomenon is known as stokes shift, which finds commercial application in the fluorescent lamps [10]. The similar result has been already reported for CBD CdS thin films [10, 13]. The PL spectra exhibit the emission bands in the visible region. One band is orange emission band with the maximum around 572nm (Fig 5.a) and 575nm (Fig 5.b) and these bands are attributed to Mn^{2+} ions. The other bands are red emission bands around 698 nm, 712nm (Fig 5.a) and 700nm, 708nm, 712nm, 732nm (Fig 5.b) which would attribute to Mn^{2+} ion-pairs. The similar results were observed by Skromme et al [14].

The absorption spectra consists of a strong (broad) peak at 350nm (Fig 4.a and 4.b) and other weak peaks at 252,307,322nm (Fig 4.a), 325,330nm (Fig 4.b). These peaks correspond to the

internal d–d optical transitions of Mn^{2+} ions. The strong peak at 350nm (3.5eV) is attributed to the transition to the band edge. The band gap of γ-MnS has been estimated as 3.5eV which is the predicted bandgap of pure binary γ-MnS as reported earlier [14-15]. The emission intensity and peak energy of emission are perhaps independent of the temperature above Neel temperature (152K) [2]. At the Neel temperature (T_N) [16], MnS transforms from an antiferromagnetic structure to an ionic crystal with the ferromagnetic structure.

Skromme et al [14] reported an unambiguous and nondestructive means of determining the crystal structure of the layers, using the Mn ions as probes of the local crystal field environment. Previous works [2] reported that 1.64eV corresponds to α-MnS (octahedral) and Skromme et al [14] concluded that the peak at 2eV is attributed to β-MnS (tetrahedral). Since strong peak in the prepared CBD MnS is at around 1.7eV, it can be concluded from the Pl spectra that MnS phase is γ phase.

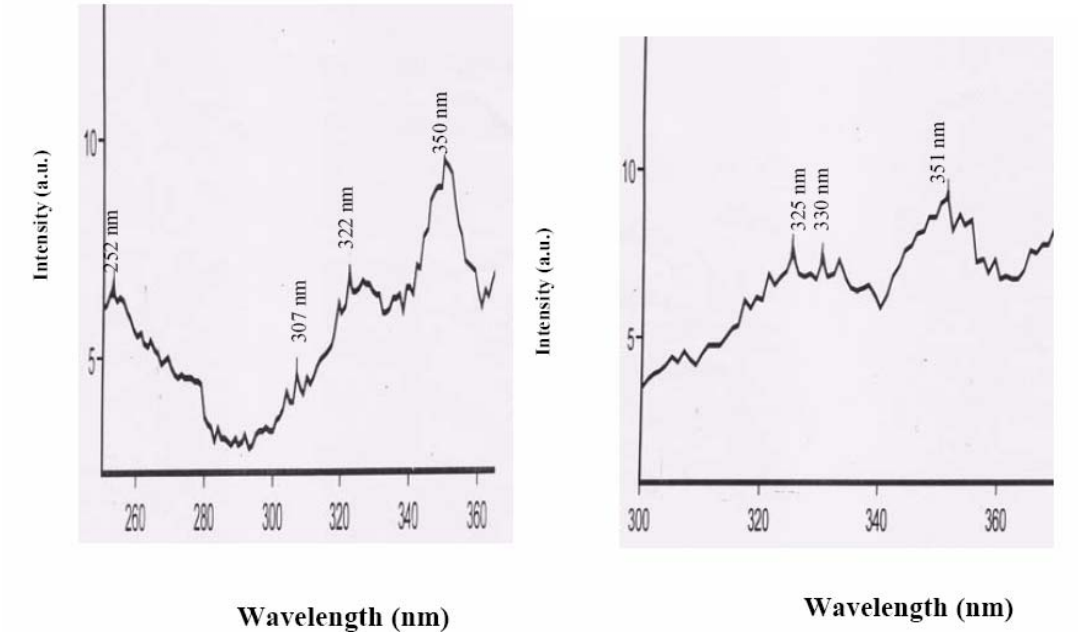

Fig 4.a Excitation Spectra of γ -MnS thin films (emission wavelength = 698nm). b. Excitation Spectra of γ -MnS thin films (emission wavelength = 700nm).

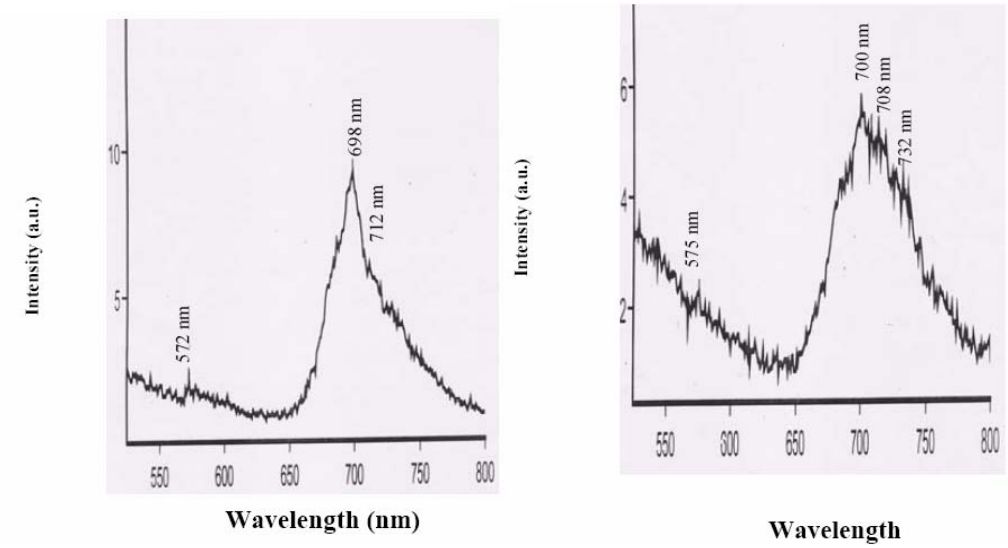

Fig. 5.a Photoluminescence Spectra of γ -MnS thin films (excitation energy = 3.5eV) 5.b Photoluminescence Spectra of γ -MnS thin films (excitation energy = 3.95eV)

c. Electrical Properties

(i) Room-temperature conductivity

The electrical measurements of the CBD γ -MnS thin films of different thicknesses were carried out in the voltage range of 5 to 20 V. Plot of the applied voltage against the resistivity (ρ) and conductivity (σ) show that the resistivity decreases and conductivity increases with increasing voltage and thicknesses. Figures (6 and 7) prove that the film has a good semi-conducting nature. The plot of the current density (J) vs. voltage was plotted in Fig 8. At lower voltages the slope of the curves was low (~0.3) and increased to 1 as the voltage increases. Therefore it can be concluded that ohmic conduction mechanism exists in CBD MnS thin films at room temperature. Fig 9 and 10 give the variation of the resistivity and conductivity with the increasing film thickness for different voltages. The decrease of ρ (Fig 9) and increase of σ (Fig 10) may be due to the improvement of crystallinity with film thickness.

(ii) High-temperature conductivity

The electrical measurements of the γ- MnS thin films were carried out in the voltage range (5-20 V) and temperature range (303K-403K) for the film of thickness 5820 Å. Plots of the observed resistivity (ρ) and conductivity (σ) with voltage show that the resistivity decreases and conductivity increases with increasing voltage and temperature Figs (11-12). Variation of log σ vs. 1000/T curves for film thickness 5820 Å is shown in Fig 13. Since the experimental data fit to the relation the high temperature conductivity is attributed due to the thermal excitation of charge carriers from grain boundaries to the neutral regions of the grains. The plot shows a unique increase in film conductivity with increase in temperature which indicates the semiconducting nature of the film [17] and the linear characteristics confirms the presence of only one type of conduction mechanism. The similar conduction mechanism has been reported for CBD Cu(I) Se, Cu(II) Se [18] and CdSe thin films [19]. Activation energy and zero-activation energy of γ-MnS thin film have been estimated using the methods reported earlier [18]. Variation of E_a with voltage is shown in Fig 14. The decrease in E_a values with applied voltage suggests that grain boundary scattering contribution reduces significantly as voltages increases. Fig15 show that conductivity pre exponential factor increases with applied voltages and the estimated high temperature electrical parameters are presented in Table 3.

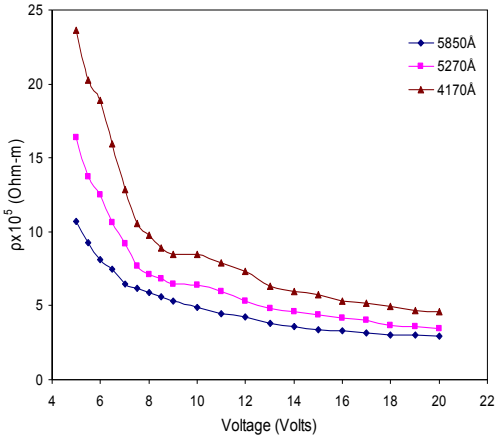

Fig.6 Plot of resistivity vs. voltage of γ MnS thin films

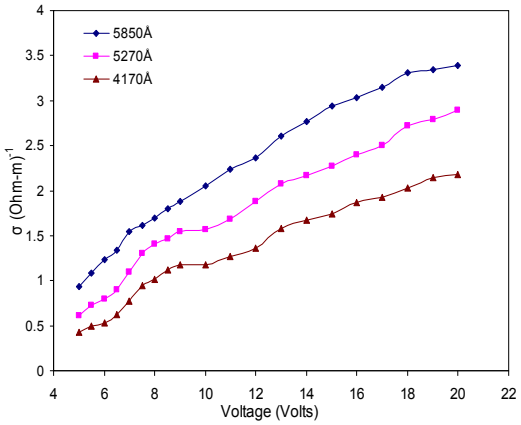

Fig 7. Room temperature variation of conductivity vs. voltage of γ -MnS thin films.

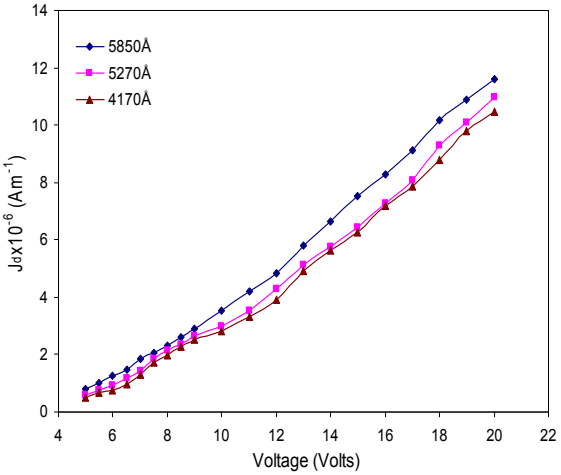

Fig 8. Variation of current density vs. voltage of γ-MnS thin films at room temperature.

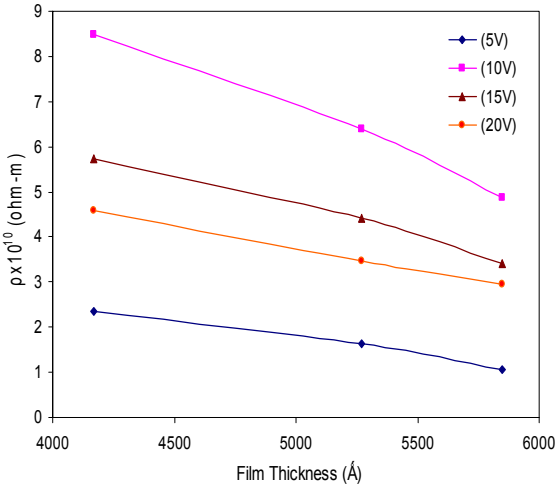

Fig 9. Variation of resistivity with film thickness for different voltages

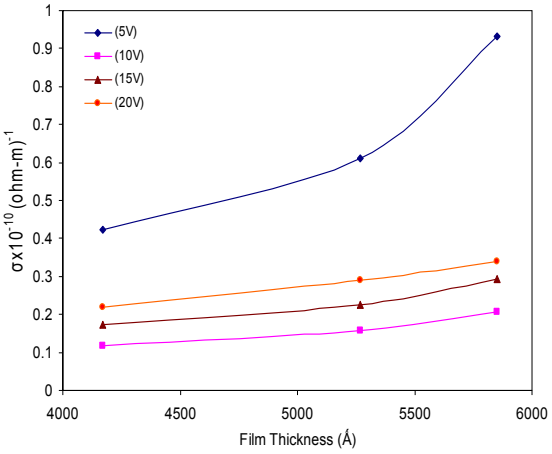

Fig 10. Variation of room- temperature conductivity with film thickness for different voltages.

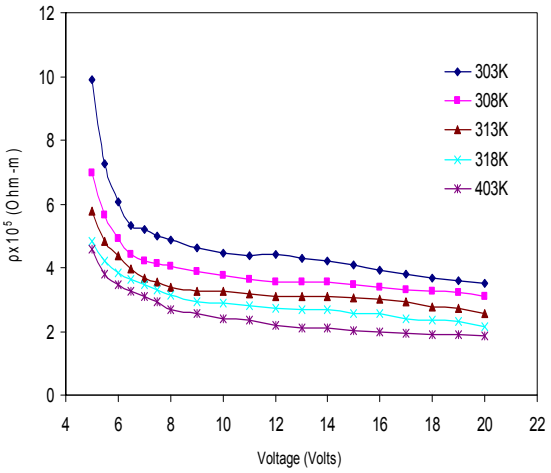

Fig 11. Plot of γ-MnS thin films resistivity vs. voltage for different temperature atthickness 5820Å.

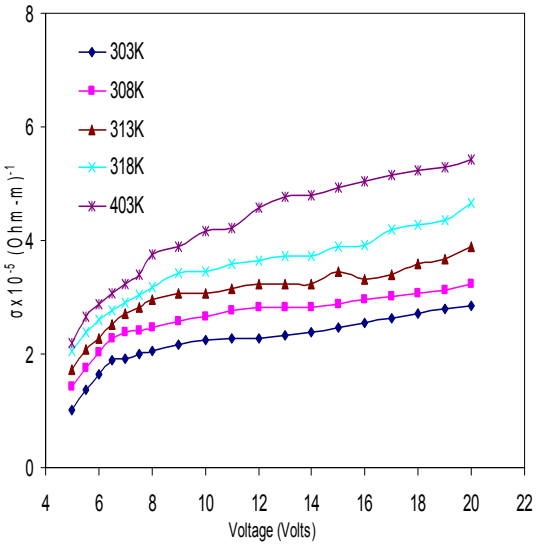

Fig 12. Plot of conductivity vs. voltage of γ- MnS thin film of thickness 5820Å at different temperatures.

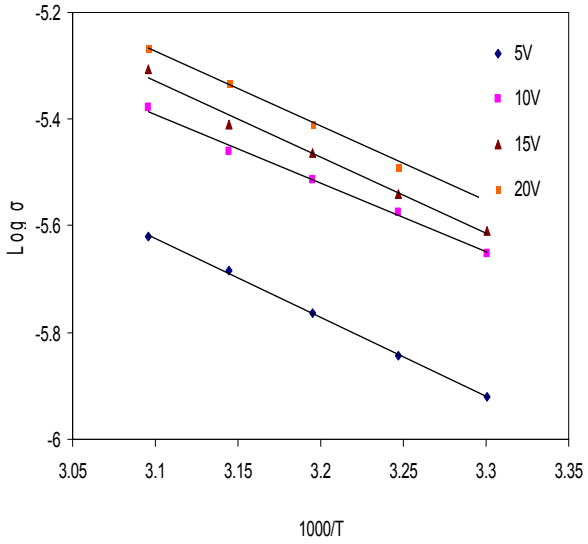

Fig 13. Plot of log σ vs. 1000/T for different voltages of γ-MnS thin film of thickness 5820Å

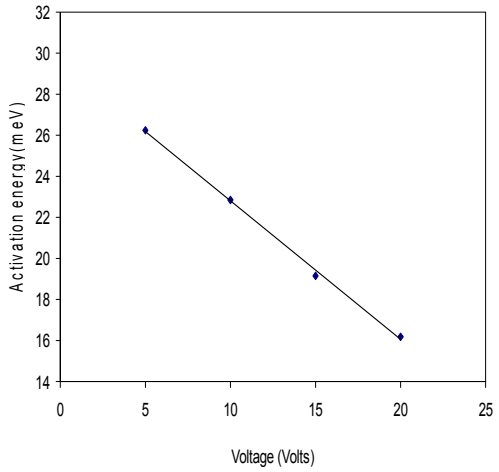

Fig 14.Plot of Activation energy (meV) vs voltage of γ- MnS thin films of thickenss 5820Å.

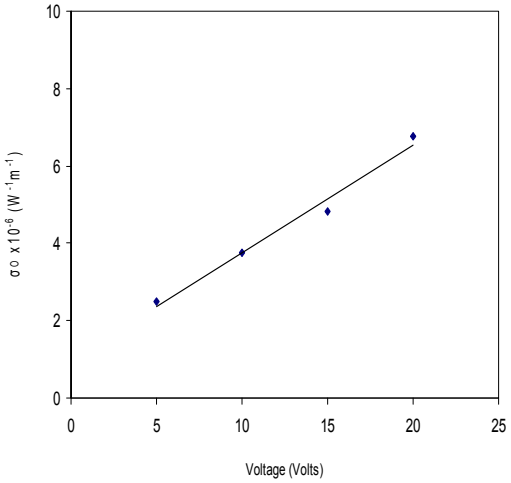

Fig 15. Plot of Voltage vs. σ_0 of γ- MnS thin films of thickness 5820Å.

Table 3. High temperature electrical parameters of CBD MnS thin films

Film thickness (Å)	Voltage (V)	σ_o x10^5 ($\Omega^{-1}m^{-1}$)	Activation energy E_a(meV)	Zero activation energy E_a(meV)
5820	5 10 15 20	2.485 3.7462 4.8306 6.7576	26.23 22.82 19.18 16.2	30

4. Conclusions

Optical investigations on γ-MnS thin films enabled to establish the type of transition as direct allowed with band gap (3.8-4eV). Room-temperature and high temperature conduction mechanism of γ- MnS thin films have been found as ohmic and ground boundary scattering respectively. The high temperature electrical parameters are also reported in this paper.

References

[1] C. D. Lokhande, A. Ennaoui, P. S. Patil, M. Gieserg, K. Diesner, H. Tributsch, Thin Solid Films, **330**, 70 (1998).
[2] D. B. Fan, X. Dong, H. Wang, Physica B, **337**, 165 (2003).
[3] O. M. Ozkendir, Y. Ufuktepe, J. Optoelectron. Adv. Mater. **7**(5), 2655 (2005).
[4] S. Biswas, S. Kar, Journal of Crystal Growth 284, 129 (2005).
[5] R. L. Gunshor, A. V. Nurmikko, Semiconductor and Semimetals, 44, Academic New York, 1997.
[6] D. B. Fan, H. Wang, Y. C. Zhang, J. Cheng, B. Wang, H. Yan, Materials Chemistry and Physics, **80**, 44 (2003).
[7] S. A.Mayen – Hernandez, Journal of Crystal Growth, **256**, 12 (2003).
[8] I. Oider-Juarez, P. Garcia-Jimenez, Materials Research Bulletin, **37**, 1749 (2002).
[9] C. Gűműş, C.Ulutaş R.Esen, Thin Solid Films **1-2**, 1 (2005).
[10] D. B. Fan, H. Wang, Y. C. Zhang, J. Cheng, B. Wang, H. Yan, Surface Review Letters, **11**, 27 (2004).
[11] M. Okajima, T. Tohda, Journal of Crystal Growth, **117**, 810 (1992).
[12] S. Prabakar, M. Dhanam, Journal of Crystal Growth, **285**, 41 (2003).
[13] J. Wilson, J. F. B. Hawkes, "Optoelectronics–An Introduction" II Edition, Prentice Hall of India Publication, New Delhi, 113 (1999).
[14] B. J. Skromme, Y. Zhang, Applied Physics Letters, **67**(18), 2690 (1995).
[15] S. Mochizuki, N. Takayama, Journal of Physics: Condensed Matter **3**, 2729 (1991).
[16] D. R. Huffman, R. L. Wild, Physical Review B, **156**, 989 (1967).
[17] V. M. Bhuse, P. P. Hankare, K. M. Garadkar, A. S. Khomane, Materials Chemistry and Physics, **80**, 82 (2003).
[18] P. K. Manoj, M. Dhanam, Rajiv. R. Prabhu, Journal of Crystal Growth, **280,** 425 (2005).
[19] M. Dhanam, R. Rajeev Prabhu, P. K. Manoj, Materials Chemistry and Physics, **107**, 289 (2008).